Scientia Iranica C (2018) 25(6), 3345–3353

Sharif University of Technology
Scientia Iranica
Transactions C: Chemistry and Chemical Engineering
http://scientiairanica.sharif.edu

$CuO/WO_3/TiO_2$ photocatalyst for degradation of phenol wastewater

F. Akhlaghian* **and A. Najafi**

Department of Chemical Engineering, Faculty of Engineering, University of Kurdistan, Sanandaj, Iran.

Received 29 September 2016; received in revised form 25 November 2017; accepted 23 June 2018

KEYWORDS
$CuO/WO_3/TiO_2$;
Phenol degradation;
Photocatalysis;
Sol-gel combustion method;
Sunlight.

Abstract. $CuO/WO_3/TiO_2$ photocatalyst was prepared by applying the sol-gel combustion method. It was characterized by X-Ray fluorescence spectroscopy, X-Ray diffraction, X-Ray photoelectron spectroscopy, porosimetry, and scanning electron microscopy techniques. The activity of $CuO/WO_3/TiO_2$ was investigated for the photocatalytic degradation of phenol wastewater. Operating conditions of batch experiments, such as initial concentration of phenol, photocatalyst dose, amount of H_2O_2, and pH, were optimized. Rate constants of the pseudo first-order reaction for several photocatalysts were determined (TiO_2: 0.0054 min^{-1}, WO_3/TiO_2: 0.0071 min^{-1}, CuO/TiO_2: 0.0118 min^{-1}, $CuO/WO_3/TiO_2$: 0.0621 min^{-1}). The $CuO/WO_3/TiO_2$ had the best performance, and its rate constant was 11.5 times greater than TiO_2. The $CuO/WO_3/TiO_2$ activity was considerable under sun light. The activity of $CuO/WO_3/TiO_2$ for 4-chlorophenol and 3-phenyl-1-propanol degradation was also successful.

1. Introduction

Phenol and its derivatives are organic pollutants that penetrate in water sources through the effluent of oil shale processing, petroleum refining, and chemical industries [1]. Because of their toxicity and carcinogenic properties, phenolic compounds are very dangerous for the environment and human health [1,2]. Heterogeneous photocatalysis is a water treatment method that uses ultraviolet (UV) light with semiconductors and has a major advantage of complete conversion of organic pollutants to CO_2, H_2O, and mineral acids [3,4].

Titania is the most famous photocatalyst that enjoys chemical and biochemical stability, low cost, and photoactivity [5,6]. Many methods are used to improve photocatalytic activity of titania, such as doping and immobilization on a support [5]. Nakano et al. [7] put TiO_2/SiO_2 photocatalyst into inquiry. Lorret et al. [8] synthesized tungsten doped titania, and found that its photocatalytic activity depends on the tungsten content and its precursor. Jeon et al. [9] prepared N-doped titania, and showed that N-doped titania had better photocatalytic activity than commercial titania P25 under visible light irradiation. In a study conducted by Luenloi and his associates [10], TiO_2 coated acrylic sheets were used as a catalyst for photodegradation of phenol. Dougna et al. [11] deposited TiO_2 on cellulose paper, stainless steel, and conducting glass. They showed that titania deposited on glass had the highest photocatalytic activity. Akhlaghian and Sohrabi [12,13] prepared Fe_2O_3/TiO_2 and CuO/TiO_2 photocatalyts through the sol-gel method and investigated their photocatalytic activities.

In this work, $CuO/WO_3/TiO_2$ was synthesized by the sol-gel combustion method to increase the photocatalytic activity of titania. The photocatalytic

*. *Corresponding author. Tel: + 98 87 33664600; Fax: +98 87 33668513*
E-mail address: akhlaghianfk@gmail.com (F. Akhlaghian)

doi: 10.24200/sci.2018.20611

activity of $CuO/WO_3/TiO_2$ was investigated for phenol and its derivatives degradation.

2. Materials and methods

2.1. Materials

The materials used include titanium isopropoxide (98%), tungstic acid (98%), copper (II) nitrate (99%), urea (99.5%), nitric acid (65%), hydrogen peroxide (30%), and phenol (99%). All of them were purchased from Merck Company. The distilled water was double distilled and prepared in the Research Laboratory of Chemical Engineering Department.

2.2. Synthesis of $CuO/WO_3/TiO_2$

The sol-gel combustion method was used. Titanium isopropoxide was the precursor of titania. Distilled water was added to the titanium isopropoxide. The molar ratio of titanium isopropoxide to water reached 1:100. Then, the solution was mixed at a constant rate at 85°C for 2 h. Nitric acid was added to the solution. The molar ratio of water to nitric acid became 1:0.07. Tungstic acid was added at this stage. After mixing at 85°C for 2 h, urea and copper (II) nitrate were added, and the molar ratio of urea to nitrate was three. The mixture was agitated under reflux at a constant rate at 85°C for 24 h. The obtained gel was dried in an oven at 100°C for 24 h. The dried gel was heated in an open muffle furnace at 400°C for a few minutes; at this temperature, urea combustion took place. The catalyst calcination progressed in a closed muffle furnace to 600°C for 2 h. The synthesized powder was crushed and sieved to mesh size of 60-90 μm [12,14-16].

2.3. Characterization

The chemical analysis of the photocatalyst was determined by X-Ray Fluorescence spectrometer Philips PW2404. X-Ray Diffractometer Philips X'Pert MPD was used to determine the crystalline degree of the sample. The X-Ray diffractometer was equipped with Co k_α radiation at 40 kV and 40 mA. The XRD patterns were collected from 10-80° in 2θ at a scan rate of 0.2°/s. The specific surface area and porosity were obtained using micrometrics ASAP 2010. Before measuring nitrogen adsorption, the catalyst was degassed at 300°C for 6 h. The MIRA3 TESCAN scanning electron microscope was used to assess the surface morphology of the catalyst. X-Ray photoelectron spectra were obtained by applying a VG Microtech XR3E2 spectrometer equipped with Al k_α (1486.6 eV) X-Ray source. UV-Vis spectrometer T80+ from PG Company was used for measuring phenol concentration.

2.4. Batch experiments

Phenol wastewater, phenol solution with the concentration of 200 ppm, photocatalyst and hydrogen peroxide were mixed. Then, the experiment was done under UV irradiation in the photoreactor. The photoreactor consisted of UV lamp, Pyrex beaker, and magnetic stirrer shielded in a chamber by aluminum foil to prevent the outside light interface. The UV lamp intensity was 242.36 mW/cm^2. At the end, the mixture was centrifuged, and the absorbance of the solution was measured at 270 nm using T80+ spectrometer. The experiment was repeated with the blank. The blank conditions were similar to the sample with no photocatalyst. The phenol degradation was calculated by:

$$\%\text{Phenol degradation} = 100 \times \left(\frac{A_0 - A}{A_0}\right), \qquad (1)$$

in which A_0 and A are the blank and sample absorbance, respectively [12,17].

3. Results and discussion

3.1. Optimization of the photocatalyst

First, WO_3 load of the photocatalyst was optimized. WO_3/TiO_2 catalysts were prepared by adding different amounts of tungstic acid. The synthesized WO_3/TiO_2 photocatalysts were applied for phenol degradation. Figure 1 shows the best WO_3/TiO_2 photocatalyst ($2.1\%WO_3/TiO_2$). When WO_3 amount was low, WO_3 acted as an effective center for electron-hole generation. The generated electron and hole were transferred to different surface sites; they reacted with adsorbed species and improved the photocatalytic activity. When WO_3 exceeded the optimum amount, the photocatalytic activity decreased due to dilution of the most active TiO_2 phase via the less active phase [8].

Figure 2 shows the effect of Cu load on phenol degradation. The ratio of WO_3 to TiO_2 is the same as the optimized catalyst of Figure 1. It was observed that increasing the amount of Cu load to 28.11% increased

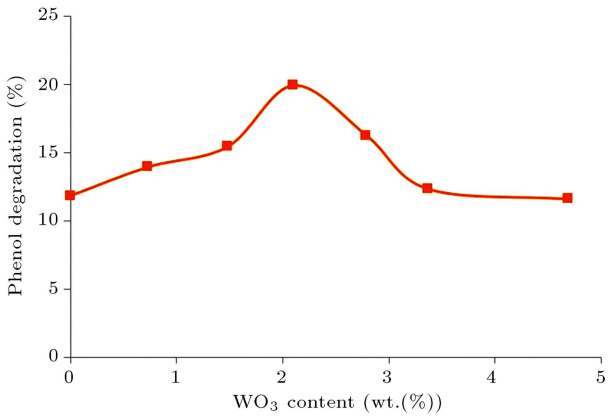

Figure 1. Effect of WO_3 content on phenol photocatalytic degradation in operating conditions: catalyst dose of 0.5 g/L, H_2O_2 amount of 587.6 mmol/L, and UV irradiation for 2 h.

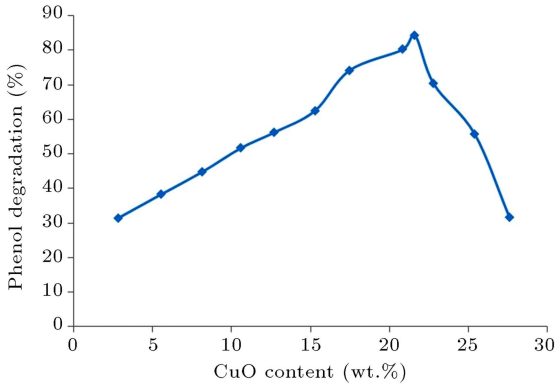

Figure 2. Effect of CuO content on phenol photocatalytic degradation in operating conditions: catalyst dose of 0.5 g/L, H_2O_2 amount of 587.6 mmol/L, and UV irradiation for 1 h.

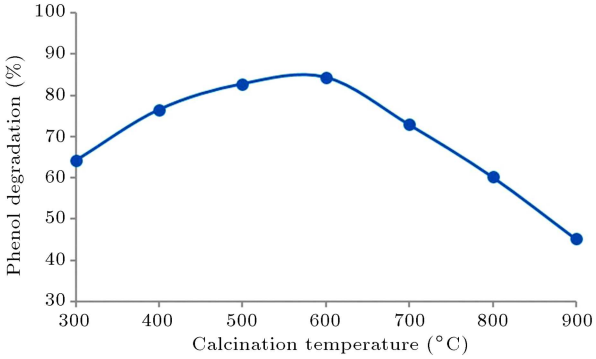

Figure 3. Effect of catalyst calcination temperature on phenol photocatalytic degradation in operating conditions: catalyst dose of 0.5 g/L, H_2O_2 amount of 587.6 mmol/L, and UV irradiation for 1 h.

active sites; Cu acts as a trapper of electrons and prevents electron-hole recombination, consequently increasing the activity of the catalyst. After Cu load reaches 28.11%, the catalyst cannot increase the phenol degradation, because Cu acts as recombination centers at high loads [18,19].

The effect of calcination temperature on the photocatalytic activity is shown in Figure 3. The highest photocatalytic activity belongs to the calcination temperature of 600°C. At a temperature higher than 600°C, the photocatalytic activity decreased, which can be attributed to a decrease in specific surface area [8,20]. At a temperature below 600°C, raising temperature increased the formation of anatase crystalline phase, improving the photocatalytic activity [8,20].

3.2. Characterization

The chemical analysis of optimized catalyst was determined by X-Ray Fluorescence spectrometry (XRF). Its composition was 28.11%CuO/2.1%WO_3/TiO_2.

Figure 4 shows X-Ray Diffraction (XRD) of TiO_2, WO_3/TiO_2, and $CuO/WO_3/TiO_2$. The XRD pattern of TiO_2 showed peaks at 32.13°, 42.13°, 45.81°, 48.29°,

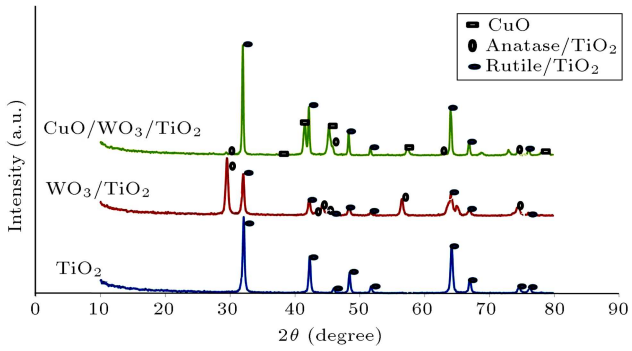

Figure 4. X-Ray diffraction patterns of TiO_2, WO_3/TiO_2, and $CuO/WO_3/TiO_2$.

51.77°, 63.97°, 47.37°, and 76.05° attributed to rutile phase (JCPDS File No. 21-1276). The XRD pattern of WO_3/TiO_2 addition to previous peaks showed peaks at 29.41°, 43.13°, 44.17°, 45.13°, 56.49°, and 74.37° related to the formation of anatase phase (JCPDS File No. 21-1272). The peaks related to WO_3 were not identified due to low amount of WO_3. WO_3 effect in the reduction of anatase phase transformation to rutile phase was observed. In the XRD pattern of $Cu/WO_3/TiO_2$, peaks attributed to CuO were observed at 37.93°, 41.53°, 45.25°, and 57.41°(JCPDS File No. 48-1548).

The nitrogen adsorption/desorption isotherm of $CuO/WO_3/TiO_2$ is represented in Figure 5(a). According to the shape of nitrogen adsorption/desorption isotherm and IUPAC classification, $CuO/WO_3/TiO_2$ photocatalyst was mesoporous and of type II. The hysteresis type of it was H3. These solid types consisted of agglomerates of particles forming slit-shaped pores (plates or edges of particles like cubes) with non-uniform size and shape [21]. Figure 5(b) shows the multimodal pore size distribution and a decrease in the prevalence of the pores as pore diameter increases. The specific surface area, pore average volume, and diameter are given in Table 1.

The images of Scanning Electron Microscopy (SEM) of TiO_2, WO_3/TiO_2, and $CuO/WO_3/TiO_2$ are provided in Figure 6. SEM images in Figure 6(a) and 6(b) show that the grains' size of WO_3/TiO_2 is smaller than TiO_2. SEM image of $CuO/WO_3/TiO_2$ in Figure 6(d) depicts brilliant spots, which are copper (II) oxide particles, and they were drawn to the surface of the catalyst. The nanosize of copper (II) oxide grains is marked in Figure 6(c).

Table 1. The specific surface area, average pore volume, and average pore diameter.

Specific surface area (m^2/g)	Average pore volume (cm^3/g)	Average pore diameter (nm)
41.1431	0.014916	14.2972

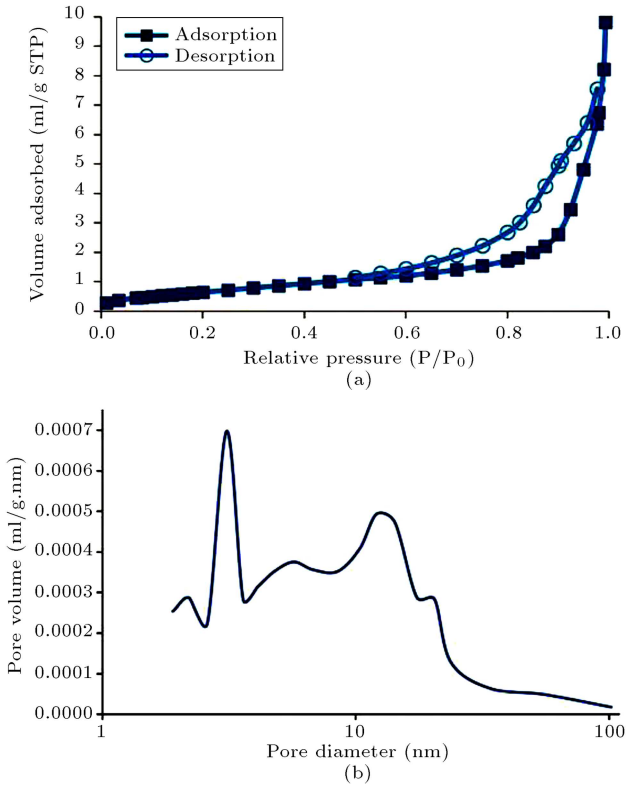

Figure 5. (a) Liquid nitrogen adsorption/desorption isotherm of $CuO/WO_3/TiO_2$. (b) Pore size distribution according to BJH desorption of $CuO/WO_3/TiO_2$ catalyst.

X-Ray Photoelectron Spectroscopy (XPS) diagram of $CuO/WO_3/TiO_2$ in the range of 450-470 eV is displayed in Figure 7(a). The diagram has two peaks at 457.58 eV and 463.8 eV binding energies. These peaks were related to Ti 2p3 and Ti 2p1, respectively [22,23]. Figure 7(b) shows the XPS diagram in the range of 30-42 eV. $CuO/WO_3/TiO_2$ photocatalyst had a shouldered peak with two edges at 35.28 and 37.6 eV binding energies attributed to W 4f7 and W 4f5, respectively. W 4f7-5 appeared as a shouldered peak due to its overlap with Ti 3p at 32.6 eV. W 4f7-5 peaks were in the range of 32.7-34 eV binding energy in $W^{4+}$and were in the range of 35.7-37.8 eV binding energy in W^{6+}. In $CuO/WO_3/TiO_2$, W 4f7-5 peaks were in the range of 34.918-37.90 eV corresponding to W^{6+}. Therefore, in $CuO/WO_3/TiO_2$, tungsten was in the complete oxidation form (+6), and its compound was WO_3 [24,25]. Figure 7(c) shows the XPS diagram in the range of 927-950 eV binding energy. $CuO/WO_3/TiO_2$ had two peaks in this range: one at 933.48 eV as a result of copper (I) oxide and copper (II) oxide peaks in the range of 932.189 and 933.958 eV binding energies, respectively. This peak was attributed to Cu 2p. The other peak in 942.681 eV binding energy corresponded to Cu^{2+} satellite peak in the range of 940.06-943 eV, hence confirming the formation of copper (II) oxide and no formation of copper (I) oxide [26].

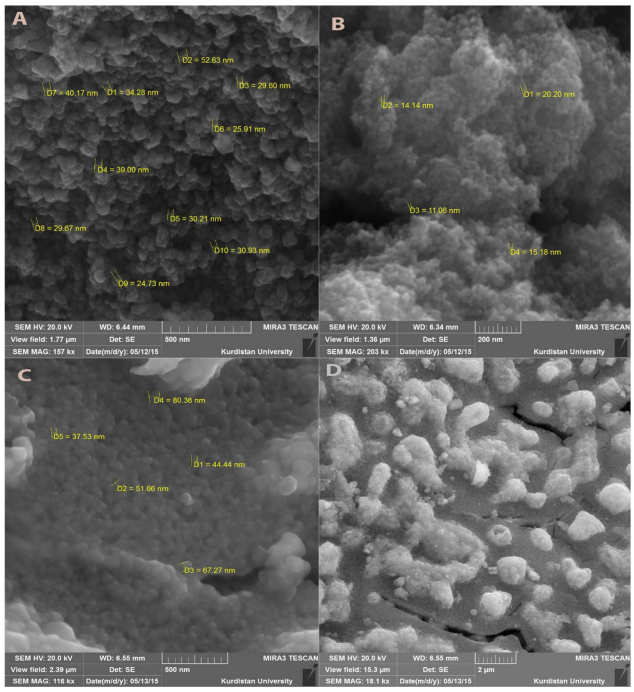

Figure 6. SEM images of the photocatalyst: (a) TiO_2, (b) WO_3/TiO_2, and (c-d) $CuO/WO_3/TiO_2$.

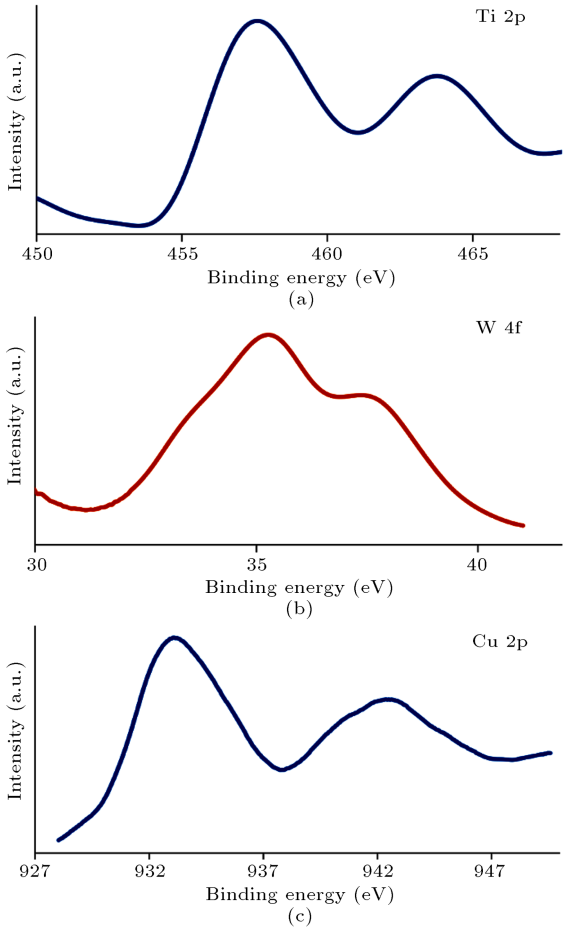

Figure 7. XPS spectra of $CuO/WO_3/TiO_2$: (a) Ti 2p, (b) W 4f, and (c) Cu 2p.

3.3. Optimization of the operating conditions

The operating conditions, including phenol initial concentration, $CuO/WO_3/TiO_2$ dosage, H_2O_2 amount, and pH, were optimized. Figure 8(a) shows that phenol solution with initial concentration of 200 ppm has the highest degradation. At concentrations higher than 200 ppm, the occupation of active sites by phenol molecules and insufficient ·OH radicals decreased phenol degradation [17].

In Figure 8(b), the optimum photocatalytic dosage is 0.75 g/L. At dosage more than 0.75 g/L, the turbidity of the suspension increases, causing light scattering, and the light reaching the catalyst active sites decreases [27].

The optimum amount of H_2O_2 is 563.6 mmol/L (Figure 8(c)). At low amounts of H_2O_2, hydroxyl radicals were small in H_2O_2 degradation; therefore, phenol degradation was small. At high amounts of H_2O_2, H_2O_2 molecules reacted with hydroxyl radicals; therefore, the hydroxyl radicals and, then, the phenol degradation decreased [17,28].

In a mild acidic condition, TiO_2 adsorbed H^+ ion and became positively charged. The electrostatic attraction made the phenol molecules be adsorbed on the positively charged catalyst surface, and the photocatalyst activity increased. At a high pH, high concentration of OH^- deactivated ·OH. Reaction of ·OH with OH^- produced $\cdot OH_2$. The reaction of $\cdot OH_2$ with phenol was very low. At a high pH, more radical-radical reactions occurred, and the phenol degradation decreased [17,28]. According to Figure 8(d), the optimum pH is 6.0 for photocatalytic phenol degradation.

3.4. Kinetics of the photocatalyst

The most common kinetics model for photocatalytic reaction is Langmuir-Hinshelwood model [17]:

$$r = -\frac{dC}{dt} = k\left(\frac{KC}{1+KC}\right), \tag{2}$$

where r is the reaction rate (ppm/min), k is the rate constant of the photocatalytic reaction (ppm/min), K is the adsorption constant (ppm^{-1}), and C is the phenol concentration (ppm). At low phenol concentration (KC≤1), KC is negligible compared to 1. Integration of Eq. (2) under these assumptions gives:

$$-\ln\left(\frac{C}{C_0}\right) = k_{app}t, \tag{3}$$

where C_0 is the initial concentration of phenol, and k_{app} is the apparent constant. Figure 9 shows the photocatalytic activities of several photocatalysts, whose phenol degradation kinetic model obeyed the pseudo first-order reaction. Table 2 shows the apparent rate constants of the photocatalysts. The addition of tungsten oxide and copper (II) oxide improves the photocatalytic activity.

Figure 10 shows the schematic of electrons and holes transfer for binary catalysts WO_3/TiO_2 and CuO/TiO_2 as well as ternary catalyst $CuO/WO_3/TiO_2$ for the photodegradation of phenol wastewater. As

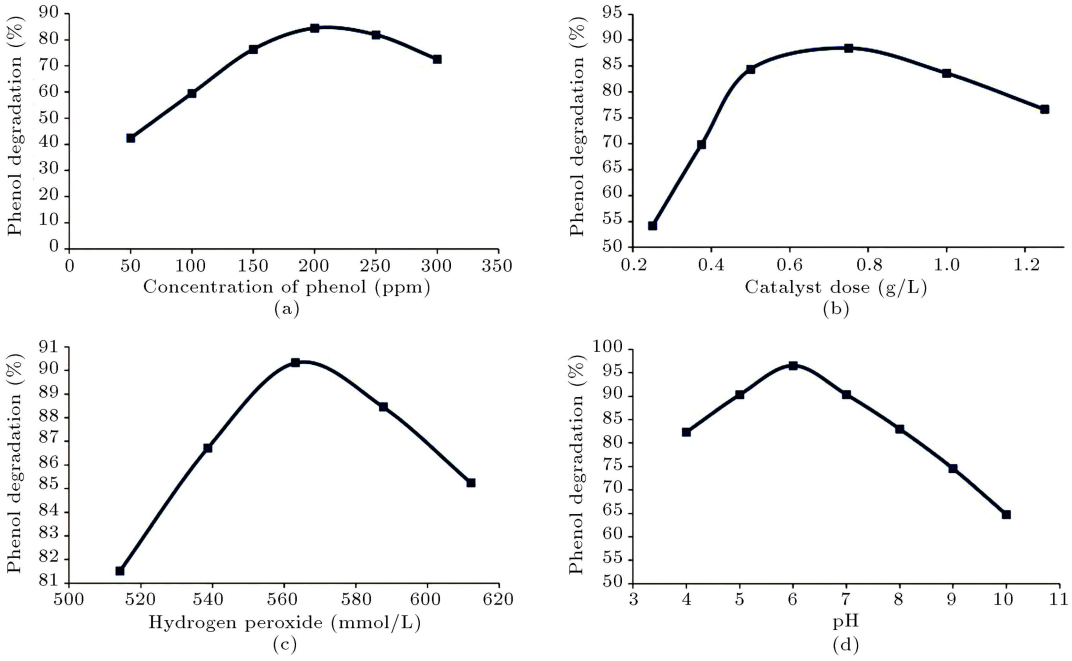

Figure 8. Optimization of operating conditions for phenol degradation: (a) Effect of phenol initial concentration, (b) effect of catalyst dose, (c) effect of H_2O_2 amount, and (d) effect of pH; all the experiments were done under UV irradiation for 1 h.

shown in Figure 10(a), the CB (Conduction Band) and VB (Valence Band) edges of WO_3 are located at −5.24 eV and −2.54 eV, respectively [29]. The CB and VB edges of TiO_2 are located at −4.21 eV and −1.01 eV, respectively [29]. The UV irradiation excited the electrons of WO_3 CB and transferred them to TiO_2 CB. The holes were transferred in the opposite direction from TiO_2 VB to WO_3 VB. The photo-generated electrons and holes were used by scavengers for the degradation of phenol. Figure 10(b) shows the representation of excitation and separation of electrons and holes for CuO/TiO_2, which is completely similar to those for WO_3/TiO_2. In the case of ternary catalyst $CuO/WO_3/TiO_2$, the UV irradiation excited the electrons of WO_3 and CuO CBs and transferred them to TiO_2 CB. Holes migrated in the opposite direction from TiO_2 VB to WO_3 and CuO VBs. The excited CB electrons of WO_3 also migrated to CuO CB; however, the holes of CuO VB were not able to migrate to WO_3 VB due to the locations of WO_3 VB edge (higher value of WO_3 VB edge), as shown in Figure 10(c). Disability of CuO VB holes for migration to WO_3 VB increased the holes of VBs, and electrons of CBs, retarding the electron-hole recombination reaction, increased the photocatalytic activity [8,30].

Table 2. Apparent rate constant for photocatalytic degradation of phenol.

Catalyst	Apparent rate constant $(min)^{-1}$	R^2
TiO_2	0.0052	0.9759
$2.1\%WO_3/TiO_2$	0.0071	0.9739
$28.11\%CuO/TiO_2$	0.0114	0.9954
$28.11\%CuO/2.1\%WO_3/TiO_2$	0.0621	0.9919

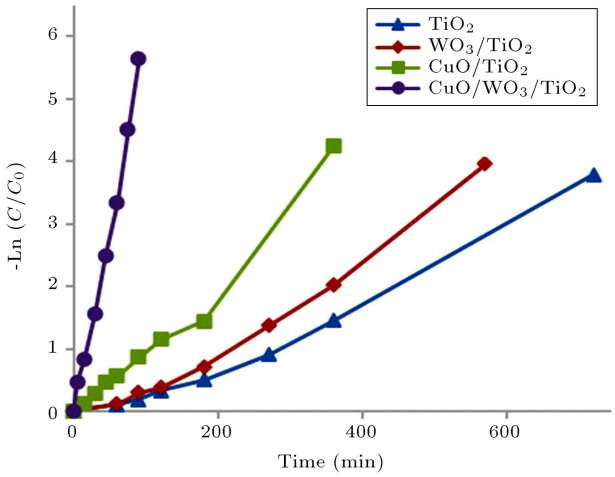

Figure 9. Pseudo first-order reaction kinetics for phenol photodegradation in operating conditions: phenol initial concentration of 200 ppm, catalyst dosage of 0.75 g/L, and H_2O_2 amount of 563.16 mmol/L.

3.5. Effect of other lights

Figure 11 compares the $CuO/WO_3/TiO_2$ activities under UV, sun, and visible light irradiation. The

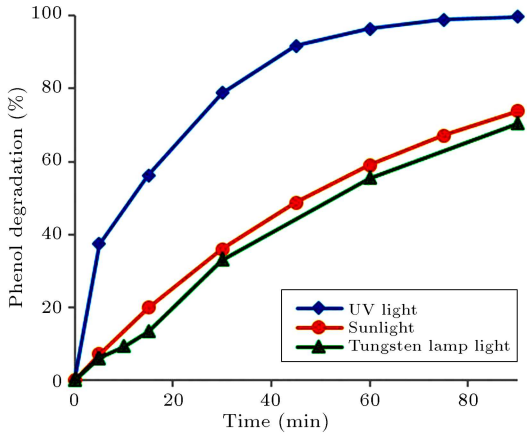

Figure 11. Effect of different lights on photocatalytic activity of $CuO/WO_3/TiO_2$ in operating conditions: phenol initial concentration of 200 ppm, catalyst dosage of 0.75 g/L, and H_2O_2 amount of 563.16 mmol/L.

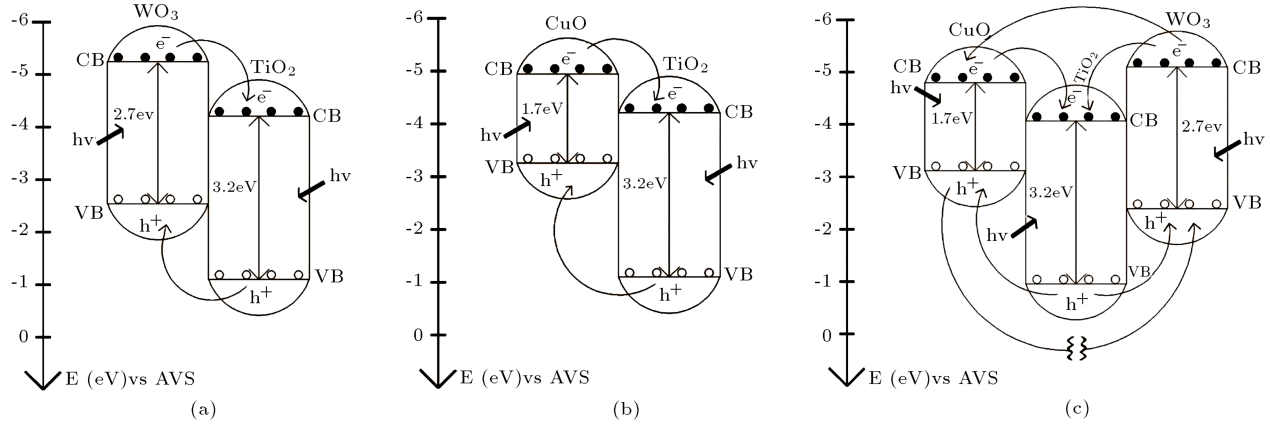

Figure 10. Schematic representation of electron-hole transfer process for phenol degradation in (a) WO_3/TiO_2, (b) CuO/TiO_2, and (c) $CuO/WO_3/TiO_2$.

measurement of sunlight photocatalytic activity was on the sunny day of July 15, 2015 in Sanandaj in the afternoon. The incandescent tungsten lamp (194 mW/cm^2) was used as the source of visible light. The rate constants of phenol degradation were 0.0621, 0.0149, and 0.0138 min^{-1} under UV, sun, and tungsten lamp light irradiation, respectively. Phenol degradation rates under sun and tungsten lamp light were considerable, although they were smaller than that under UV light irradiation.

3.6. Removal of other organic pollutants

The degradation of organic pollutants, 4-chlorophenol and 3-phenyl-1-propanol, was investigated using $CuO/WO_3/TiO_2$. The results showed that degradation obeyed pseudo first-order kinetics (Figure 12). The rate constants are provided in Table 3. These findings indicate that $CuO/WO_3/TiO_2$ is an effective photocatalyst for degradation of phenolic compounds.

4. Conclusions

$CuO/WO_3/TiO_2$ photocatalyst was prepared using the sol-gel combustion method. WO_3 and CuO loads of the photocatalyst were determined through XRF: 28.11%CuO/2.1%WO_3/TiO_2. X-Ray results showed titania in rutile and anatase phases and confirmed the existence of copper (II) oxide. The hysteresis was of type II and H3. SEM images showed the effects of CuO and WO_3.

This study investigated the phenol degradation kinetics of several photocatalysts (TiO_2, WO_3/TiO_2, CuO/TiO_2, and $CuO/WO_3/TiO_2$). The results revealed that all obeyed the pseudo first-order kinetics. The rate constants of photocatalysts showed that $CuO/WO_3/TiO_2$ was the most effective. The $CuO/WO_3/TiO_2$ activity was measured under sun and, then, was compared to that under UV light. The findings show good activity of the catalyst under sunlight. Other phenolic compounds, such as 4-chlorophenol and 3-phenyl-1-propanol, were also degraded effectively by $CuO/WO_3/TiO_2$ photocatalyst. It can be concluded that $CuO/WO_3/TiO_2$ is a very effective photocatalyst for degradation of phenolic pollutants under UV and sunlight.

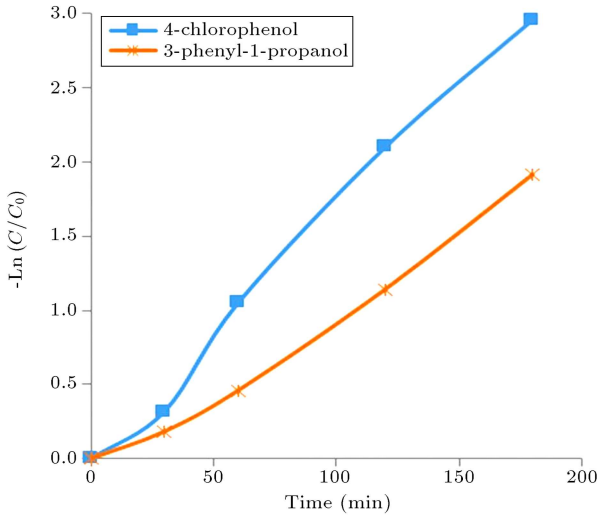

Figure 12. Pseudo first-order reaction kinetics for 4-chlorophenol and 3-phenyl-1-propanol photodegradation in operating conditions: pollutant initial concentration of 200 ppm, catalyst dosage of 0.75 g/L, and H_2O_2 amount of 563.16 mmol/L.

Table 3. Apparent rate constant for $CuO/WO_3/TiO_2$ for degradation of phenolic compounds.

Pollutant	Degradation after 3h UV irradiation	Apparent rate constant (min^{-1})	R^2
4-Chlorophenol	94.8%	0.017	0.9929
3-Phenyl-1-propanol	85.13%	0.0108	0.9890

Acknowledgements

The financial support of the University of Kurdistan is gratefully acknowledged.

References

1. Choquette-Labbé, M., Shewa, W.A., Lalman, J.A., and Shanmugan, S.R. "Photocatalytic degradation of phenol and phenol derivatives using a Nano-TiO_2 catalyst: Integrating quantitative and qualitative factors using response surface methodology", *Water*, **6**, pp. 1785-1806 (2014).
2. Malakootian, M., Mansoorian, H.J., Alizadeh, M., and Baghbanian, A. "Phenol removal from aqueous solution by adsorption process: Study of the nanoparticles performance prepared from aloe vera and mesquite (prosopis) leaves", *Sci. Iran Trans. C.*, **24**(6), pp. 3041-3052 (2017).
3. Ray, A.K. and Beenackers, A.A.C.M. "Novel photocatalytic reactor for water purification", *AIChE J.*, **44**(2), pp. 447-483 (1998).
4. Cruz, M., Gomez, C., Duran-Valle, C.J., Pastrana-Martnez, L.M., Faria, J., Silva, A.M.T., Faraldos, M., and Bahamonde, A. "Bare TiO_2 and graphene oxide TiO_2 photocatalysts on the degradation of selected pesticides and influence of the water matrix", *Appl. Surf. Sci.*, **416**, pp. 1013-1021 (2017).
5. Ngamsopasiriskun, C., Charnsethikul, S., Thachepan, S., and Songsasen, A. "Removal of phenol in aqueous solution by nanocrystalline TiO_2/activated carbon composite catalyst", *Kasetsart J. (Nat. Sci.)*, **44**, pp. 1176-1182 (2010).
6. Sohrabi, S., Akhlaghian, F. "Surface investigation and

catalytic activity of iron-modified TiO_2", *J. Nanostruct. Chem.*, **6**, pp. 93-102 (2016).

7. Nakano, K., Obuchi, E., Takagi, S., Yamamoto, R., Tanizki, T., Taketomi, M., Eguchi, M., Ichida, K., Suzuki, M., and Hashimoto, A. "Photocatalytic treatment of water containing dinitrophenol and city water over TiO_2/SiO_2", *Sep. Purif. Technol.*, **34**, pp. 67-72 (2004).
8. Lorret, O., Francová, D., Waldner, G., and Stelzer, N. "W-doped titania nanoparticles for UV and visible-light photocatalytic reactions", *Appl. Catal. B: Environ.*, **91**, pp. 39-46 (2009).
9. Jeon, J.W., Kim, J.R., and Ihm, S.K. "Continuous one-step synthesis of N-doped titania under supercritical and subcritical water conditions for photocatalytic reaction under visible light", *J. Phys. Chem. Solids*, **71**, pp. 608-611 (2010).
10. Luenloi, T., Chalermsinsuwan, B., Sreethawong, T., and Hinchiranan, N. "Photodegradation of phenol catalyzed by TiO_2 coated on acrylic sheets: Kinetics and factorial design analysis", *Desalination*, **274**, pp. 192-199 (2011).
11. Dougna, A.A., Gombert, B., Kodom, T., Djaneye-Boundjou, G., Boukari, S.O.B., Leitner, N.K.V., and Bawa, L.M. "Photocatalytic removal of phenol using titanium dioxide deposited on different substrates: Effect of inorganic oxidants", *J. Photoch. Photobio. A*, **30**, pp. 67-77 (2015).
12. Akhlaghian, F. and Sohrabi, S. "Fe/TiO_2 catalyst for photodegradation of phenol in water", *I.J.E. Transactions A.*, **28**, pp. 499-506 (2015).
13. Sohrabi, S. and Akhlaghian, F. "Modeling and optimization of phenol degradation over copper-doped titanium dioxide photocatalyst using response surface methodology", *Process Saf. Environ.*, **99**, pp. 120-128 (2016).
14. Sedghi, A., Baghshahi, S., Riahi Nouri, N., and Barkhordari, M. "Synthesis of titanium oxide nano powder by a novel gel combustion method", *D.J. Nanomater. Biostruc.*, **6**, pp. 1457-1462 (2011).
15. Shokrani, R., Haghighi, M., Jodeiri, N., Ajamein, H., and Abdollahifar, M. "Fuel cell grade hydrogen production via methanol steam reforming over $CuO/ZnO/Al_2O_3$ nanocatalyst with various oxide ratios synthesized via urea nitrates combustion method", *Int. J. Hydrogen Energ.*, **39**, pp. 13141-13155 (2014).
16. Castaño, M.H., Molina R., and Moreno, S. "Oxygen storage capacity and oxygen mobility of Co-Mn-Mg-Al mixed oxides and their relation in the VOC oxidation reaction" *Catalysts*, **5**, pp. 905-925 (2015).
17. Nezamzadeh-Ejhieh, A., and Salimi, Z. "Heterogeneous photodegradation catalysis of o-phenylenediamine using CuO/X zeolite", *Appl. Catal. A: Gen.*, **390**, pp. 110-118 (2010).
18. Tseng, I.-H. Chang, W.C., and Wu, J.C.S. "Photoreduction of CO_2 using sol-gel derived titania and titania-supported copper catalysts", *Appl. Catal. B: Environ.*, **37**, pp. 37-48 (2002).
19. Tseng, I.-H. and Wu, J.C.S. "Chemical states of metal-loaded titania in the photoreduction of CO_2", *Catal. Today*, **97**, pp. 113-119 (2004).
20. Yu, J.-G., YU, H.-G., Cheng, B., Zhao, X.-Y., Yu, J.C., and Ho, W.-K. "The effect of calcination temperature on the surface microstructure and photocatalytic activity of TiO_2 thin films prepared by liquid phase deposition", *J. Phy. Chem. B*, **107**, pp. 13871-13879 (2003).
21. Leofanti, G., Padovan, M., Tozzola, G., and Venturelli, B. "Surface area and pore texture of catalysts", *Catal. Today*, **41**, pp. 207-219 (1998).
22. Milošev, I., Kosec, I., and Strehblow, H.-H. "XPS and EIS study of the passive film formed on orthopaedic Ti-6Al-7Nb alloy in Hank's physiological solution", *Electrochim. Acta*, **53**, pp. 3547-3558 (2008).
23. Suñol, J.J. Bonneau, M.E., Roué, L., Guay, D., and Schulz, R. "XPS surface study of nanocrystalline Ti-Ru-Fe materials", *Appl. Surf. Sci.*, **158**, pp. 252-262 (2000).
24. Occhiuzzi, M., Cordischi, D., Gazzoli, D., Valigi, M., and Heydorn, P.C. "WOx/ZrO_2 catalysts Part 4. Redox properties as investigated by redox cycles, XPS and EPR", *Appl. Catal. A: Gen.*, **269**, pp. 169-177 (2004).
25. Dupin, J.C., Gonbeau, D., Martin-Litas, I., Vinatier, Ph., and Levasseur, A. "Amorphous oxysulfide thin films MOySz (M=W, Mo, Ti) XPS characterization: structural and electronic peculiarities", *Appl. Surf. Sci.*, **173**, pp. 140-150 (2001).
26. Ethiraj, A.S., and Kang, D.J. "Synthesis and characterization of CuO nanowires by a simple wet chemical method", *Nanoscale Res. Lett.*, **7**, pp. 1-5 (2012).
27. Pouretedal, H.R., Norozi, A., Keshavarz, M.H., and Semnani, A. "Nanoparticles of zinc sulfide doped with manganese, nickel and copper as nanophotocatalyst in the degradation of organic dyes", *J. Hazard. Mater.*, **162**, pp. 674-681 (2009).
28. Ahmed, S., Rasul, M.G., Martens, W.N., Brown, R., and Hashib, M.A. "Heterogeneous photocatalytic degradation of phenols in wastewater: A review on current status and developments", *Desalination*, **261**, pp. 3-18 (2010).
29. Xu, Y., and Schoonen, M.A.A. "The absolute energy positions of conduction and valence bands of selected semiconducting minerals", *Am. Mineral.*, **85**, pp. 543-556 (2000).
30. Mageshwari, K., Nataraj, D., Pal, D., Sathyamoorthy, R., and Park, J. "Improved photocatalytic activity of ZnO coupled CuO nanocomposites synthesized by reflux condensation method", *J. Alloy. Compd.*, **625**, pp. 362-370 (2015).

Biographies

Faranak Akhlaghian received her PhD degree in Chemical Engineering from Tarbiat Modares University in 2010. Now, she is an Assistant Professor at University of Kurdistan, Sanandaj, Iran. Her research interests are heterogeneous catalysis and modeling of chemical processes.

Azade Najafi received her MSc degree in Chemical Engineering from University of Kurdistan in 2016. Her research interest is heterogeneous photocatalysis.